Growth of c-axis oriented ZnO nanowires from aqueous solution: The decisive role of a seed layer for controlling the wires' diameter

G. Kenanakis [a,b,c,d], D. Vernardou [a,d,e], E. Koudoumas [a,f], N. Katsarakis [a,c,d,*]

[a] Center of Materials Technology and Laser, School of Applied Technology, Technological Educational Institute of Crete, 710 04 Heraklion, Crete, Greece
[b] Department of Chemistry, University of Crete, 710 03 Heraklion, Crete, Greece
[c] Institute of Electronic Structure and Laser, Foundation for Research & Technology-Hellas, P.O. Box 1527, Vassilika Vouton, 711 10 Heraklion, Crete, Greece
[d] Science Department, School of Applied Technology, Technological Educational Institute of Crete, 710 04 Heraklion, Crete, Greece
[e] Department of Materials Science and Technology, University of Crete, 710 03 Heraklion, Crete, Greece
[f] Department of Electrical Engineering, Technological Educational Institute of Crete, 710 04 Heraklion, Crete, Greece

ARTICLE INFO

ABSTRACT

ZnO nanowires were grown from an aqueous solution at low temperature (95 °C) on Corning glass and silicon (1 0 0) substrates. It turns out that the deposition of a thin ZnO seed layer on the substrates prior to the chemical growth is crucial for obtaining c-axis oriented ZnO nanowires with controllable dimensions. The nanowires' diameter increases with the grain size of the ZnO seed layer. On the other hand, aqueous solution growth on bare substrates leads to the formation of flowerlike nanostructures, consisting of nanorods, with no preferred growth orientation. The dimensions and morphology of these complex nanostructures depend mainly on growth time. Furthermore, the complex ZnO nanostructures do not show high transmittance, while the nanowires are highly transparent in the visible part of the spectrum.

1. Introduction

Zinc oxide (ZnO) is a well-studied transparent direct wide band-gap semiconductor (E_g=3.37 eV) with a large exciton binding energy (~60 meV), which allows efficient excitonic emission at room temperature (RT) [1,2]. ZnO nanowires, in particular, have attracted a great attention in the last years due to their applications in sensors, cantilevers as well as in optoelectronic devices such as light-emitting diodes and excitonic solar cells [3,4]. Law et al. [5] have applied ZnO vertically oriented nanowires in dye-sensitized solar cells and reported a full Sun efficiency of 1.5%. Ravirajan et al. have fabricated hybrid polymer/ZnO photovoltaic devices with vertical oriented nanorods, resulting in a power conversion efficiency of 0.2%. It turns out that the

morphology and dimensions of the ZnO nanorods strongly affect charge recombination and device performance [6].

Different chemical and physical methods have been applied in the last years for creating a large variety of ZnO nanostructures with shapes ranging from nanowires to nanobelts and even nanosprings [3]. For instance, high temperature vapor–liquid–solid (VLS) growth with the use of catalysts [7,8], pulsed laser deposition [9], electrochemical deposition in porous membranes [10], metal vapor transport using Zn sources [11], physical vapor transport using ZnO and graphite powders [12], chemical vapor deposition using zinc acetylacetonate hydrate [13], thermal oxidation of ZnS [14], metalorganic chemical vapor deposition (MOCVD) using diethylzinc and O_2 or N_2O as precursors [15] and aqueous solution growth [16–18] have been reported amongst other techniques.

Aqueous solution approaches for the growth of ZnO nanostructures are considered advantageous, compared with other methods, mainly due to low growth temperature and good potential for large-scale production. Vayssieres et al. [16,17] have first demonstrated the growth of ZnO oriented micro- and

nanorods on conducting glass substrates and Si substrates at 95 °C. Andrés-Vergés et al. [18] had though already reported the formation of prisms, needles and spherulitic aggregates from the hydrolysis of zinc nitrate and zinc chloride in the presence of hexamethylenetetramine depending on reactant concentration, pH and temperature. Tian et al. [19] have later introduced a low-temperature synthetic route for the fabrication of complex and oriented ZnO nanostructures, in which citrate anions were used to control crystal morphology. In the last years, many groups have reported the growth of highly oriented ZnO nanowires and other nanostructures from aqueous solutions [20–28]. It is currently believed that a ZnO seed layer is needed to initialize the uniform growth of oriented nanowires from aqueous solutions. To our knowledge, there have been no up-to-date systematic studies showing how the presence of a seed layer affects the ZnO nanostructures' crystallinity and morphology. It is however of great importance to be able to accurately control the morphology and dimensions of the as-grown ZnO nanostructures. This is a prerequisite for the application of nanowires' arrays in solar cells and light-emitting devices.

In this work, we thoroughly investigate the growth of highly oriented ZnO nanowires on Corning glass and silicon (1 0 0) substrates from aqueous solution according to the approach of Andrés Vergés et al. [18] and Vayssieres et al. [17]. The aim of our study is to explore systematically the seed layer's influence on the ZnO nanostructures' crystallinity, morphology and dimensions. We demonstrate that the occurrence of a ZnO seed layer on the substrate is necessary in order to produce highly c-axis oriented ZnO nanowires with controllable dimensions. The diameter of the ZnO nanowires can be tuned by varying the grain size of the seed layer. On the other hand, direct growth from an aqueous solution on bare Corning glass and silicon (1 0 0) substrates leads to the formation of complex ZnO nanostructures with no preferred growth orientation. The dimensions and morphology of these complex nanostructures depend mainly on growth time.

2. Experimental part

Our growth procedure consists of two steps. In the first step, ZnO thin films with a thickness of 60 and 140 nm, which were subsequently used as seed layers for the aqueous solution growth of ZnO nanostructures, were prepared via the sol–gel/spin coating technique [29]. Zinc acetate dehydrate was first dissolved in a mixture of 2-methoxy ethanol and monoethanolamine at room temperature (RT). The concentration of zinc acetate was 0.75 mol/l and the molar ratio of monoethanolamine to zinc acetate was kept at 1:1. The resultant solution was stirred for 1 h at 60 °C to yield a homogeneous, clear and transparent solution using a magnetic stirrer. The seed layers were spin-coated a day after the solution was prepared. The precursor solution was dropped onto Corning glass and silicon (1 0 0) substrates, which were then spinned at 3000 rpm for 20 s. After processing, the substrates were baked at 350 °C for 10 min to evaporate the solvent and to remove the organic component in the films. The procedure was repeated 3 or 6 times. The films were then annealed in air at 600 °C for 60 min. The thickness of the films was measured using a stylus profilometer (alpha-step 100, Tencor).

In the second step, ZnO nanostructures were grown on Corning glass and Si (1 0 0) substrates from an equimolar (0.01 M) aqueous solution of $Zn(NO_3)_2 \cdot 6H_2O$ and $C_6H_{12}N_4$ [16–18,28]. The solution and the substrates, bare or pre-coated with ZnO seed layers prepared via sol–gel, were placed in Pyrex glass bottles with autoclavable screw caps and heated at 95 °C for 2 and 5 h in a regular laboratory oven. After each induction time, the samples were thoroughly washed with MilliQ water to eliminate residual

salts or amino complexes, and dried in air at the same temperature. All substrates used were cleaned using a Piranha solution ($H_2SO_4/H_2O_2=3/1$), rinsed with MilliQ water and dried under N_2 gas flow.

The crystal structure of the ZnO nanostructures was determined by X-ray diffraction (XRD) using a Rigaku (RINT 2000) diffractometer with Cu Ka X-rays, while their surface morphology was studied with a field emission scanning electron microscope (FE-SEM, JEOL JSM-7000F) and an atomic force microscope (AFM) in tapping mode (Digital Instruments–Nanoscope IIIa). The surface roughness (RMS) of the samples was determined by the SPIP 3.3.5.0 from Image Metrology. Finally, UV–vis transmission spectra were recorded using a Perkin–Elmer Lambda 950 spectrometer over the wavelength range 190–1100 nm.
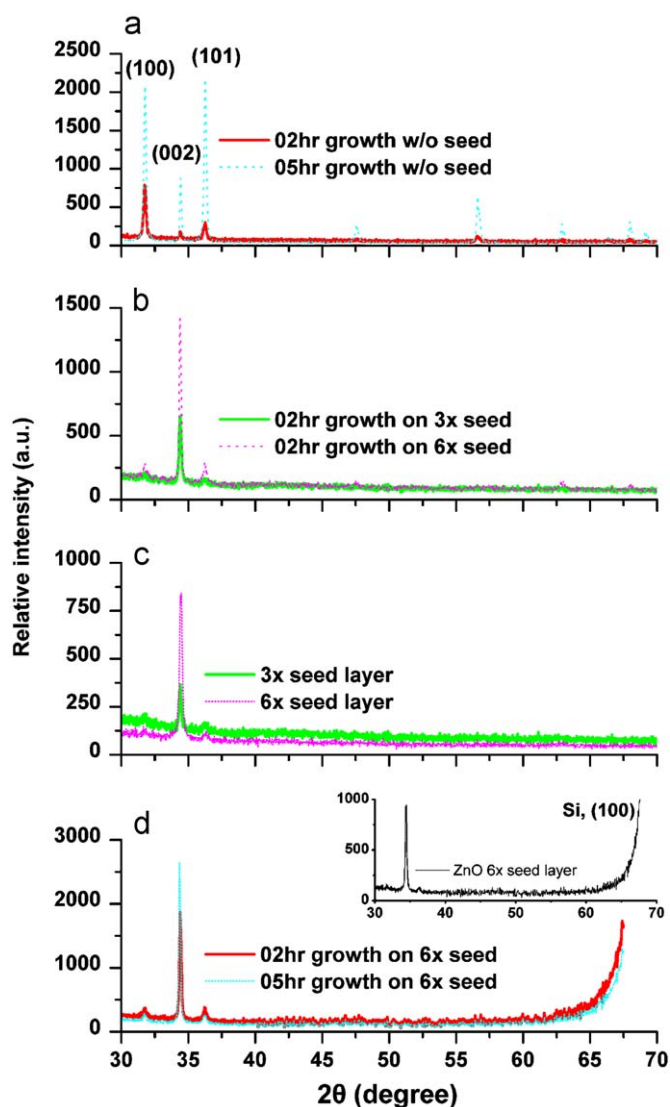
Fig. 1. XRD patterns of (a) ZnO samples grown by aqueous solution growth on bare Corning glass substrates for 2 h (red curve) and 5 h (light-blue dashed curve), (b) ZnO samples grown by aqueous solution growth for 2 h on Corning glass substrates with a 3-layered (60-nm-thick, green curve) and a 6-layered (140-nm-thick, magenta dashed curve) ZnO seed layer, (c) 3-layered (60-nm-thick, green curve) and 6-layered (140-nm-thick, magenta dashed curve) ZnO seed layers deposited via sol–gel on Corning glass substrates, and (d) ZnO samples grown by aqueous solution growth on silicon (1 0 0) substrates with a 6-layered (140-nm-thick) ZnO seed layer for 2 h (red curve) and 5 h (light-blue dashed curve). In the inset of (d) the XRD pattern of a 6-layered (140-nm-thick) ZnO seed layer deposited on Si (1 0 0) via sol–gel is presented. (For interpretation of the references to colour in this figure legend, the reader is referred to the web version of this article.).

3. Results and discussion

Fig. 1 depicts X-ray diffraction patterns of the ZnO nanostructures deposited on Corning glass substrates by aqueous solution growth. The substrates used were either bare (Fig. 1a) or pre-coated with three or six ZnO thin layers deposited by the sol–gel/spin-coating technique (Fig. 1b and d). The thickness of the ZnO thin films is 60 and 140 nm for the three- and six-layered samples, respectively. It can be readily seen that, if no seed layer is applied onto the Corning glass substrates prior to the aqueous solution growth, all reflections corresponding to the hexagonal wurtzite P6(3)mc structure (JCPDS card file No. 36-1451) are present and there is no preferential growth orientation for neither 2 nor 5 h growth time (see Fig. 1a). On the other hand, when a ZnO seed layer, consisting of either three (60 nm) or six (140 nm) layers, is applied onto the Corning glass substrates prior to the aqueous solution growth, there is a clear preferential growth orientation of the ZnO nanostructured samples along the (0 0 2) crystallographic direction, i.e. perpendicular to the Corning glass substrates (2 h growth, Fig. 1b). This preferential growth orientation is directly related to the presence of the ZnO seed layers [21]. As it can be observed in Fig. 1c, both the three- and six-layered thin films exhibit the ZnO wurtzite hexagonal structure and grow preferentially along the (0 0 2) direction. Therefore, they

indeed act as seed layers and assist the preferential growth of the chemically grown ZnO nanostructures along the c-axis, i.e. the (0 0 2) crystallographic direction. Moreover, it can be observed that the samples deposited by aqueous solution growth show much larger and sharper (0 0 2) reflections than the seed layers (Fig. 1b and c). The Full-Width at Half-Maximum (FWHM) value for the (0 0 2) peak varies between 0.205° and 0.245° for the ZnO seed layers, while it is 0.176° and 0.174° for the ZnO samples grown on a 140-nm-thick ZnO seed for 2 and 5 h, respectively. It is therefore concluded that the occurrence of a thin ZnO seed layer is crucial for the growth of well-crystalline, (0 0 2) oriented ZnO samples onto Corning glass substrates.

It is also noted that the thickness of the seed layer strongly affects the crystallinity of the ZnO samples grown from aqueous solution. In particular, the crystallinity of the ZnO nanostructured samples improves with increasing thickness of the seed layer. In the case of 2 h growth, for example, the FWHM values of the (0 0 2) peak are 0.202° and 0.176° for the samples grown on 60- and 140-nm-thick seed layers, respectively. It is furthermore observed that increasing aqueous solution growth time on a seed layer of a specific thickness leads to slightly smaller FWHM values (0.176° and 0.174° for 2 and 5 h growth time respectively on Corning glass substrates pre-coated with a 140-nm-thick ZnO seed layer). It is thus concluded that the most significant
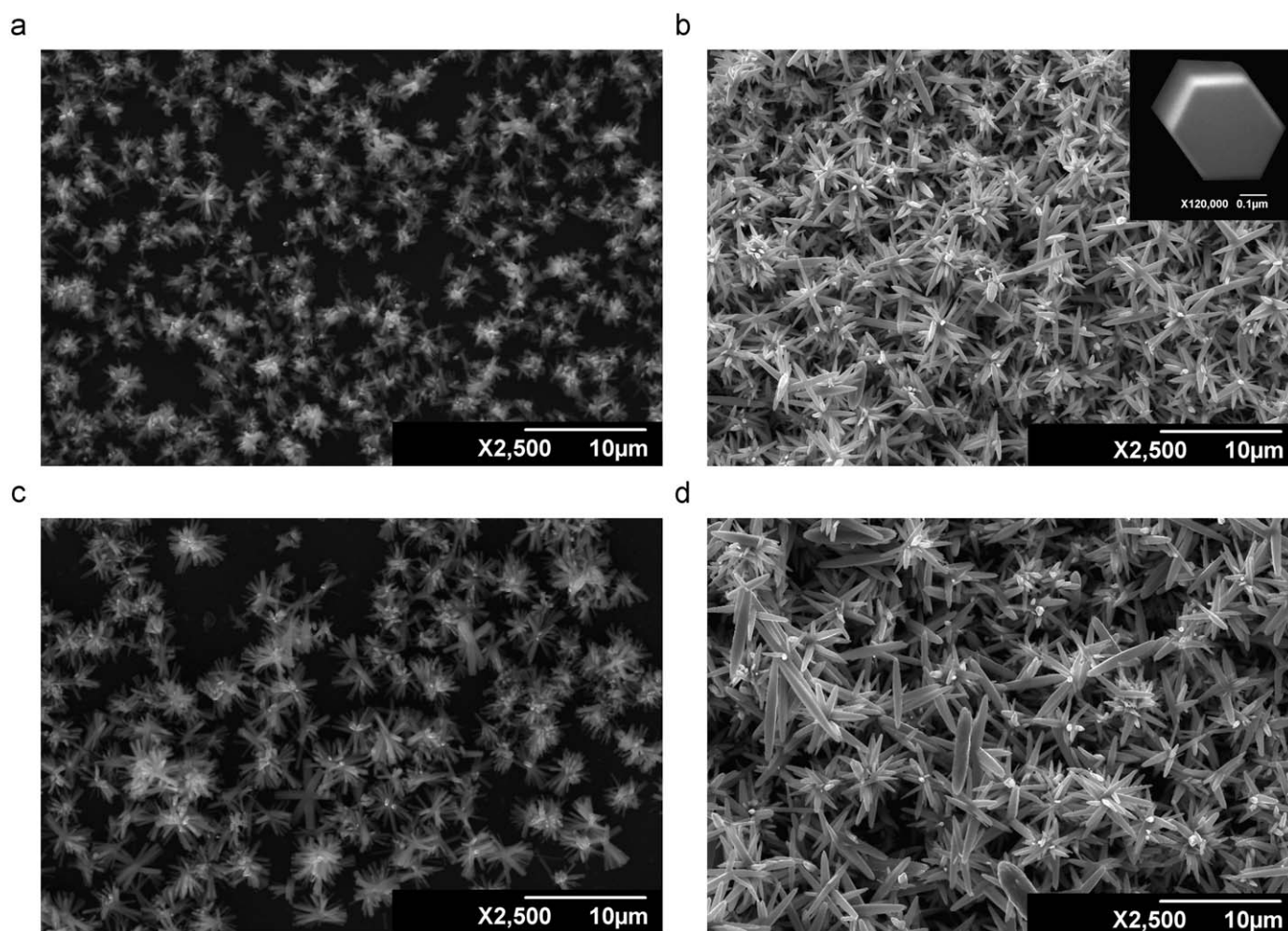
Fig. 2. SEM images of ZnO nanostructures grown by aqueous solution growth on bare Corning glass substrates for (a) 2 h and (b) 5 h, and on bare silicon (1 0 0) substrates for (c) 2 h and (d) 5 h. In the inset of (b) the hexagonal cross section of the ZnO nanorods is clearly observed.

parameter, which affects the crystallinity of the ZnO samples deposited by aqueous solution growth, is the thickness of the seed layer and not the growth time.

The same behavior is qualitatively observed for the samples grown on silicon (1 0 0) substrates. In this case, one can also observe the peaks corresponding to the Si (1 0 0) and (2 0 0) crystallographic planes (see Fig. 1d and inset herein). The FWHM values for the (0 0 2) ZnO peak are 0.181° and 0.178° for the 2 and 5 h samples grown on a 140-nm-thick ZnO seed layer, respectively. It is therefore concluded that, irrespectively of the substrate used, Corning glass or silicon (1 0 0), the presence of a seed layer leads to the formation of ZnO samples with very good crystallinity and a preferential growth orientation along the c-axis, i.e., perpendicular to the substrate.

Fig. 2a and b show SEM micrographs of ZnO samples deposited on bare Corning glass substrates for 2 and 5 h, respectively. As it can be readily observed, for 2 h growth, flowerlike microstructures occur, consisting of nanorods with a diameter ranging from 200 to 300 nm and length of ∼2–3 μm. However, the size of the flowerlike nanostructures is not uniform, while a few of single rods (diameter ∼350 nm, length ∼2–3 μm) are also present. When the growth time increases to 5 h, the flowerlike architectures develop further and become dominant with substrate coverage of ∼80%. They consist of uniform nanorods with a typical diameter of around 400–500 nm and length of several microns (∼5–6 μm). All nanorods have hexagonal cross

section (see the inset of Fig. 2b), implying the occurrence of the wurtzite ZnO crystal structure as it was also demonstrated by XRD (see Fig. 1a).

SEM micrographs of ZnO samples deposited by aqueous solution growth on bare silicon (1 0 0) substrates are depicted in Fig. 2c and d for 2 and 5 h, respectively. Flowerlike nanostructures, consisting of nanorods, occur for both periods. With increasing growth time the nanostructures become gradually larger. For 2 h growth the nanorods' diameter is 300–400 nm and their length varies from 4 to 5 μm, while in the case of 5 h growth the nanorods display a typical diameter of ∼600–700 nm and length of ∼6–8 μm. It is concluded that the ZnO nanostructured samples deposited on bare Corning glass and silicon (1 0 0) substrates by aqueous solution growth do not consist of oriented nanorods, in accordance with the XRD results which show that all reflections of the ZnO wurtzite structure are present (see Fig. 1a).

Fig. 3a and b depict SEM micrographs of the ZnO samples deposited by aqueous solution growth for 2 h on Corning glass substrates pre-coated with 60- and 140-nm-thick seed layers, respectively. It can be readily seen that these samples exhibit a totally different morphology, i.e., nanowires' arrays occur. These nanowires emerge perpendicular to the substrates applied, are quite dense and uniform, while they all display a hexagonal cross-section. These remarks are in agreement with the XRD results which clearly demonstrate that the ZnO samples deposited by
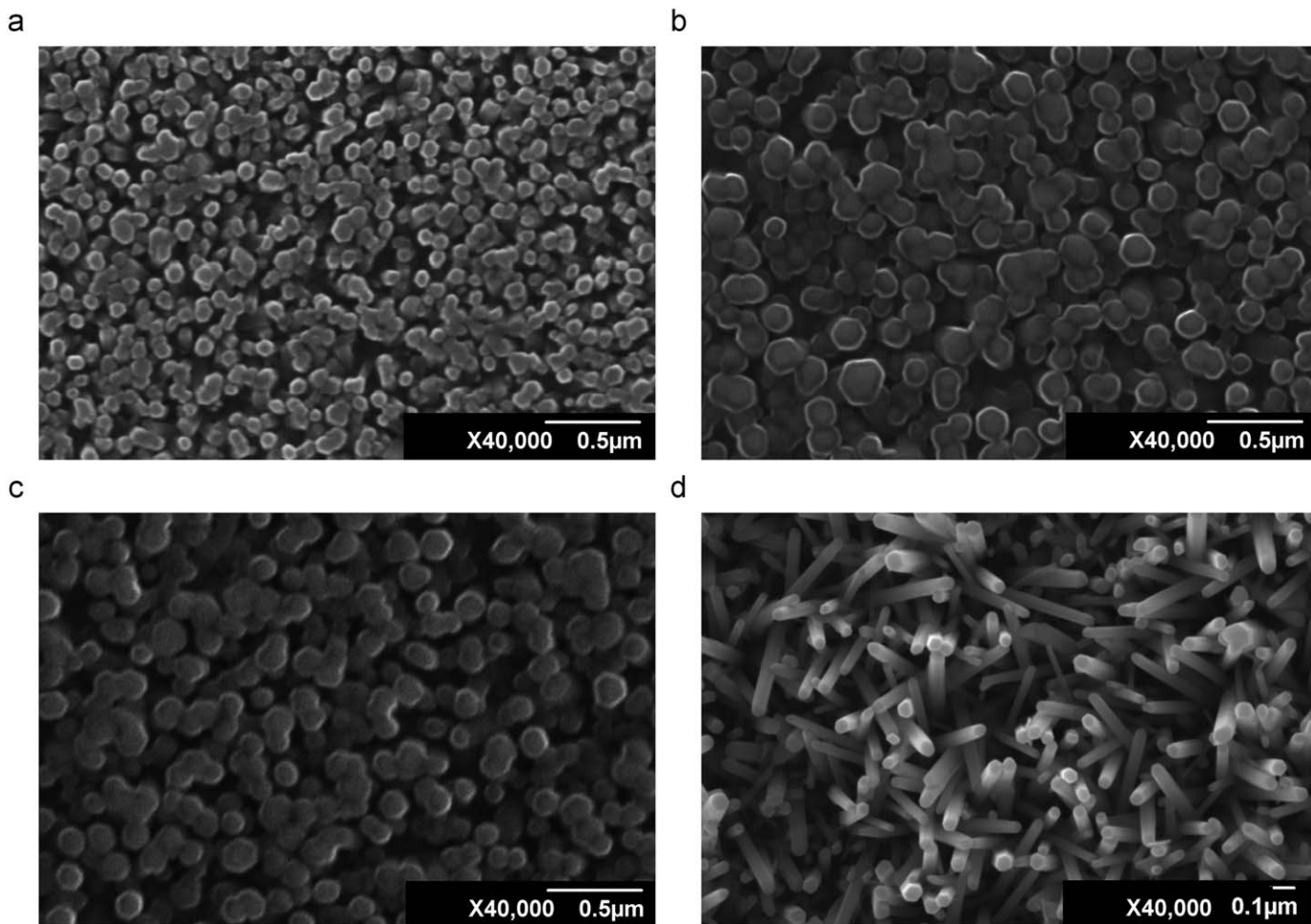
Fig. 3. SEM images of ZnO nanowires grown by aqueous solution growth for (a) 2 h on Corning glass/60-nm-thick ZnO seed layer, (b) 2 h on Corning glass/140-nm-thick ZnO seed layer, (c) 5 h on Corning glass/140-nm-thick ZnO seed layer and (d) 5 h on silicon (1 0 0)/140-nm-thick ZnO seed layer.

aqueous solution growth on pre-coated Corning glass substrates exhibit the wurtzite hexagonal crystal structure and show a preferential growth orientation along the (0 0 2) direction (see Fig. 1b and d). It is furthermore observed that the nanowires' diameter increases with the seed layer thickness. As the seed layer thickness increases from 60 to 140 nm, the wires' diameter rises from $\sim 80 \pm 10$ to $\sim 100 \pm 10$ nm. This increase in the wires' diameter is directly related to the grain size of the ZnO seed layer. The grain size as well as the roughness of the seed layers gradually increase with thickness, i.e., the number of the spin-coated layers (see Fig. 4a). As it can be seen from Fig. 4a, the grain size of the 60- and 140-nm-thick seed layers is 67 ± 4 and 92 ± 5 nm, respectively, i.e., quite close to the diameter values of the corresponding ZnO nanowires' arrays. It is therefore concluded that the occurrence of a ZnO seed layer is a prerequisite for obtaining well-oriented ZnO nanowires onto Corning glass substrates via aqueous solution growth, and that the seed layer's grain size strongly affects the ZnO nanowires' diameter, i.e., the wire diameter increases with the grain size of the seed layer. When the growth time increases from 2 to 5 h, the diameter of the nanowires remains almost constant (see Fig. 3b and c for 2 and 5 h growth on a 140-nm-thick seed layer, respectively). It thus seems that the growth time does not significantly influence the wires' diameter.

Fig. 3d displays a SEM micrograph of ZnO nanowires grown for 5 h by aqueous solution growth on a silicon (1 0 0) substrate, which was pre-coated with a 140-nm-thick ZnO seed layer. The nanowires' diameter is around 55 ± 5 nm, much smaller than that obtained on Corning glass substrates, a behavior which is directly related to the grain size of the seed layer. As it can be seen in Fig. 4b, the grain size of the 140-nm-thick seed layer deposited via sol–gel on a silicon (1 0 0) substrate is 50 ± 4 nm, which is almost the half of that on Corning glass (92 ± 5 nm). The larger grain size of the ZnO seed layer deposited on Corning glass is possibly related with better promotion of the nucleation due to the higher affinity of ZnO to Corning glass as compared to silicon (1 0 0) [30]. This higher affinity seems to also influence the growth rate, this being slightly larger in the case of Corning glass. It can be finally observed that although the nanowires are quite dense and uniform, they are not as well-aligned as the ones grown on
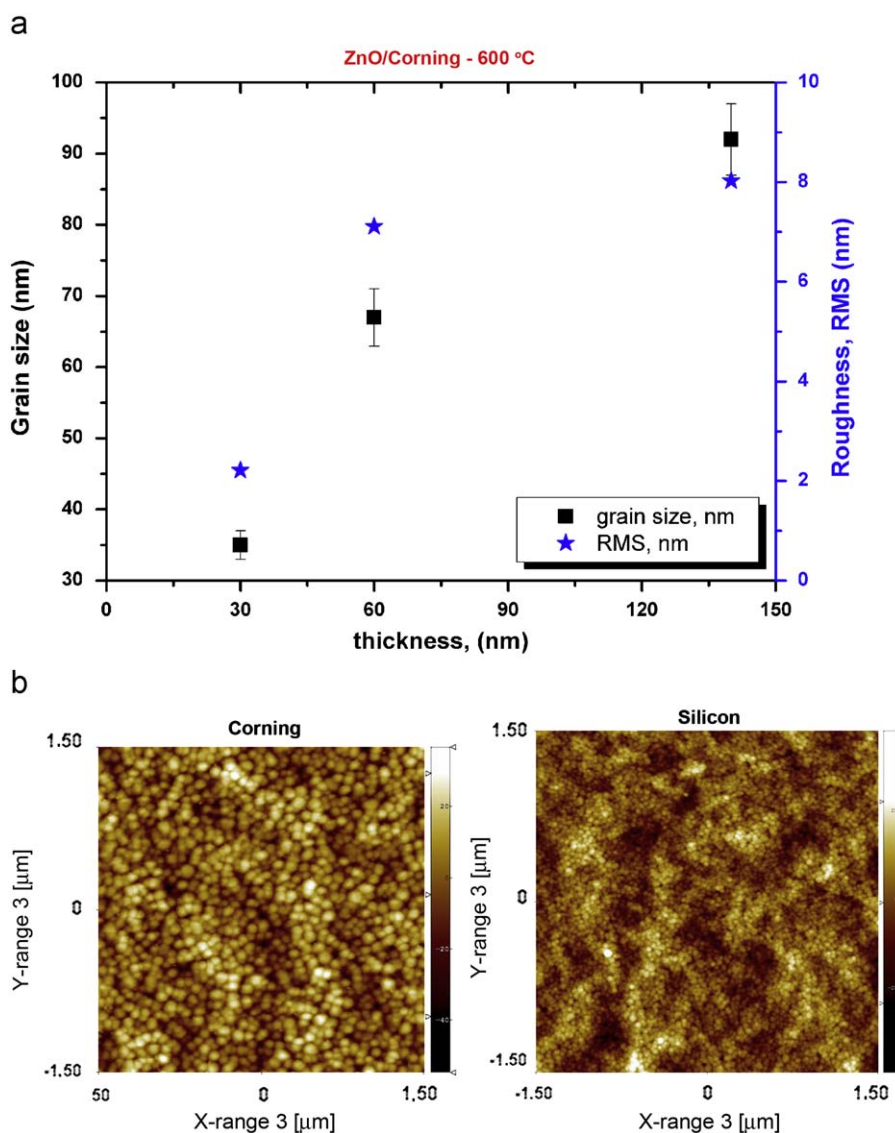
Fig. 4. (a) Grain size (black squares) and roughness (blue stars) vs. thickness of the sol–gel deposited ZnO seed layers on Corning glass annealed at 600 °C and (b) AFM images (scan size 3 μm × 3 μm) of 140-nm-thick ZnO seed layers on Corning (left) and silicon (right) substrates. (For interpretation of the references to colour in this figure legend, the reader is referred to the web version of this article.).
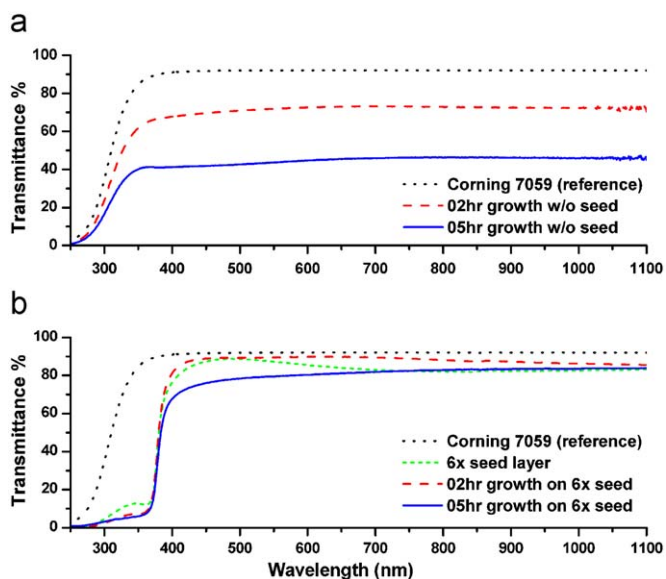
Fig. 5. Optical transmittance spectra of (a) ZnO flowerlike nanostructures grown by aqueous solution growth at 95 °C on bare Corning glass substrates for 2 h (red dashed curve) and 5 h (blue solid curve) and (b) ZnO nanowires' arrays grown on a 140-nm-thick seed layer for 2 h (red dashed curve) and 5 h (blue solid curve); the green dotted curve displays the transmittance spectrum of the 140-nm-thick ZnO seed layer deposited via sol–gel. For comparison reasons, in both (a) and (b), one can see the transmittance spectrum of bare Corning glass substrate (black dotted curve). (For interpretation of the references to colour in this figure legend, the reader is referred to the web version of this article.).

Corning glass substrates. This is probably related with the morphology of the 140-nm-thick seed layer deposited on the silicon (1 0 0) substrate [21] and is currently under further investigation.

The transmittance spectra of the ZnO nanostructures grown by aqueous solution growth on bare Corning glass substrates are presented in Fig. 5a. It is clearly observed that by increasing the growth time from 2 to 5 h, the transmittance decreases. This is most probably related to the samples' thickness and morphology. As the growth time rises from 2 to 5 h, larger nanostructures occur, the substrate coverage as well as the samples' thickness increase, and thus the transmittance falls.

In Fig. 5b the transmittance spectra of the ZnO seed layers and the nanowires' arrays are depicted. All the samples are highly transparent in the visible region and exhibit a sharp absorption band in the UV region. First, it is observed that while the ZnO nanostructures grown directly on bare Corning glass substrates are not well transparent for both 2 and 5 h growth time, i.e., they display transmittance values of almost 70% and 40%, respectively (see Fig. 5a), the nanowires deposited on substrates pre-coated with a seed layer show remarkable good transmittance in the visible part of the spectrum (90% and 80% for the ZnO nanowires deposited by aqueous solution growth over a period of 2 and 5 h, respectively, on top of a 140-nm-thick ZnO seed layer, see Fig. 5b). Moreover, it is quite interesting that the chemically grown ZnO nanowires display similar transmittance values with those observed for the ZnO seed layers alone. For example, ZnO nanowires grown for 2 h on a 140-nm-thick ZnO seed layer exhibit 90% transmittance at 600 nm, while a 140-nm-thick ZnO seed layer shows 85% transmittance at the same wavelength (see Fig. 5b). Finally, it can be noted that increasing the ZnO nanowires' growth time from 2 to 5 h leads to a decrease in transmittance from 90% to almost 80% at 600 nm, a drop, which can be attributed to the increase in the samples' thickness.

4. Conclusions

ZnO nanostructures were grown from an aqueous solution on Corning glass and silicon (1 0 0) substrates at low temperature (95 °C). The substrates used were either bare or pre-coated with a thin ZnO seed layer deposited via the sol–gel/spin-coating method. It is concluded that the presence of a ZnO seed layer is crucial for the formation of well-aligned, c-axis oriented ZnO nanowires with good crystallinity. The diameter of the nanowires increases with the grain size of the ZnO seed layer and varies between 50 and 110 nm depending on the substrate used. On the other hand, if no seed layer is applied, flowerlike nanostructures occur, consisting of nanorods with a diameter ranging from 200 to 700 nm and length of ∼2–8 μm, depending on growth time and substrate applied. In this case, all crystallographic planes exist and there is no preferred growth orientation. Finally, it is shown that the ZnO flowerlike nanostructures are not well transparent, while the ZnO nanowires' arrays show very high transmittance in the visible part of the spectrum, reaching values comparable to those of the seed layers.

References

[1] Ü. Özgür, Y.I. Alivov, C. Liu, A. Teke, M.A. Reshchikov, S. Dogan, V. Avrutin, S.J. Cho, H. Morkoç, J. Appl. Phys. 98 (2005) 041301.
[2] D.P. Norton, Y.W. Heo, M.P. Ivill, K. Ip, S.J. Pearton, M.F. Chisholm, T. Steiner, Mater. Today 7 (6) (2004) 34.
[3] Zhong Lin Wang, Mater. Today 7 (6) (2004) 26.
[4] Lukas Schmidt-Mende, Judith L. MacManus-Driscoll, Mater. Today 10 (5) (2007) 40.
[5] M. Law, L.E. Green, J.C. Johnson, R. Saykally, P. Yang, Nat. Mater. 4 (2005) 455.
[6] P. Ravirajan, A.M. Peiró, M.K. Nazeeruddin, M. Graetzel, D.D.C. Bradley, J.R. Durrant, J. Nelson, J. Phys. Chem. B 110 (2005) 7635.
[7] H. Huang, Y. Wu, H. Feick, N. Tran, E. Weber, P. Yang, Adv. Mater. 13 (2001) 113.
[8] H. Huang, S. Mao, H. Feick, H. Yan, Y. Wu, H. Kind, N. Tran, E. Weber, R. Ruso, P. Yang, Science 292 (2001) 1897.
[9] J.H. Choi, H. Tabata, T. Kawai, J. Cryst. Growth 226 (2001) 493.
[10] C. Liu, J.A. Zapien, Y. Yao, X. Meng, C.S. Lee, S. Fan, Y. Lifshitz, S.T. Lee, Adv. Mater. 15 (2003) 838.
[11] S.C. Lyu, Y. Zhang, H. Ruh, H.J. Lee, H.W. Shim, E.K. Suh, C.J. Lee, Chem. Phys. Lett. 363 (2002) 134.
[12] B.D. Yao, Y.F. Chen, N. Wang, Appl. Phys. Lett. 81 (2002) 757.
[13] J.J. Wu, S.C. Liu, J. Phys. Chem. B 106 (2002) 9546.
[14] X.T. Zhang, Y.C. Liu, L.G. Zhang, J.Y. Zhang, Y.M. Lu, D.Z. Shen, W. Xu, G.Z. Zhong, X.W. Fan, X.G. Kong, J. Appl. Phys. 92 (2002) 3292.
[15] S.W. Kim, Sz. Fujita, Sg. Fujita, Appl. Phys. Lett. 81 (2003) 5036.
[16] L. Vayssieres, Adv. Mater. 15 (2003) 464.
[17] L. Vayssieres, K. Keis, S.-E. Lindquist, A. Hagfeldt, J. Phys. Chem. B 105 (2001) 3350.
[18] M. Andrés-Vergés, A. Mifsud, C.J. Serna, J. Chem. Soc., Faraday Trans. 86 (1990) 959.
[19] Z.R. Tian, J.A. Voigt, J. Liu, B. Mckenzie, M.J. Mcdermott, M.A. Rodriguez, H. Konishi, H. Xu, Nat. Mater. 2 (2003) 821.
[20] M. Kreye, B. Postels, H.-H. Wehmann, D. Fuhrmann, A. Hangleiter, A. Waag, Phys. Stat. Sol. (c) 3 (2006) 992.
[21] Q. Li, V. Kumar, Y. Li, H. Zhang, T.J. Marks, R.P.H. Chang, Chem. Mater. 17 (2005) 1001.
[22] C. Liu, Y. Masuda, Y. Wu, O. Takai, Thin Solid Films 503 (2006) 110.
[23] L.E. Green, M. Law, D.H. Tan, M. Montano, J. Goldberger, G. Somorjai, P. Yang, Nano Lett. 5 (2005) 1231.
[24] H. Zhang, D. Yang, S. Li, X. Ma, Y. Ji, J. Xu, D. Que, Mater. Lett. 59 (2005) 1696.
[25] J. Liu, X. Huang, Y. Li, J. Duan, H. Ai, Mater. Chem. Phys. 98 (2006) 523.
[26] D. Vernardou, G. Kenanakis, S. Couris, E. Koudoumas, E. Kymakis, N. Katsarakis, Thin Solid Films 515 (2007) 8764.
[27] D. Vernardou, G. Kenanakis, S. Couris, A.C. Manikas, G.A. Voyiatzis, M.E. Pemble, E. Koudoumas, N. Katsarakis, J. Cryst. Growth 308 (2007) 105.
[28] G. Kenanakis, D. Vernardou, E. Koudoumas, G. Kiriakidis, N. Katsarakis, Sens. Actuators B: Chem. 124 (2007) 187.
[29] H. Li, J. Wang, H. Liu, H. Zhang, X. Li, J. Cryst. Growth 275 (2005) 943.
[30] S. Yamabi, H. Imai, J. Mater. Chem. 12 (2002) 3773.